Molar Mass Distribution of Linear and Branched Polyurethane Studied by Size Exclusion Chromatography

Frederic Prochazka, Taco Nicolai,* and Dominique Durand

Chimie et Physique des Matériaux Polymères, UMR CNRS,Université du Maine, 72085 Le Mans Cedex 9, France

Received February 4, 1999; Revised Manuscript Received December 20, 1999

ABSTRACT: Linear polyoxypropylene (POP) diol and star POP triol were end-linked using diisocyanate. Linear and branched polyurethanes (PU) of varying size were formed by varying the stoichiometric ratio r of isocyanate and hydroxyl groups. End-linked POP triol forms a gel for $r > 0.55$. Molar mass distributions of linear and soluble branched PU were determined using size exclusion chromatography as a function of r in the range 0−1. The fractions of the first few oligomers at different r are in good agreement with calculated values using mean field theory. Branched POP triol has a very broad molar mass distribution close to the gel point. At low degree of polymerization (DP < 10) the molar mass distribution is well described by mean field theory while for DP > 300 it is better described by the percolation model. The results imply that many earlier measurements on gel-forming systems reported in the literature were done on samples in the crossover regime.

Introduction

The polycondensation reaction of poly(oxy)propylene (POP) with a diisocyanate leads to the formation of polyurethane (PU). If we use a bifunctional POP, we obtain linear PU, while if we use a POP with higher functionality we obtain branched PU. The mean molar mass and the molar mass distribution of PU depend in both cases on the ratio of the isocyanate groups to the alcohol groups ($r = [NCO]/[OH]$), the functionality of the POP used (φ), and the reaction extent (p). If the average functionality of POP is larger than 2, a gel will be formed above a critical value of r (r_c) and of p (p_c). Ideally, when $r = 1$ and $p = 1$, the system consists of a single linear chain if $\varphi = 2$ or a perfect three-dimensional network if $\varphi > 2$. Of course, for real systems such a situation is never obtained.

Mean field theory[1−5] can be used to calculate the molar mass distribution as a function of r, φ, and p. In its most elementary form, mean field theory assumes equal reactivity of the functional groups independent of the size of the macromolecules, and it ignores effects of excluded volume interactions and cyclization. The neglect of these effects is especially important close to the gel point. Close to the gel point, the number of macromolecules with molar mass M is predicted to decrease with increasing M following a power law dependence:

$$N(M) \propto M^{-\tau} f(M/M^*) \quad M \gg M_0 \tag{1}$$

Here M_0 is the molar mass of the precursors and $f(x)$ represents the cutoff function of the power law dependence at a characteristic molar mass, M^*, proportional to the z-averaged molar mass, M_z. The polydispersity exponent τ equals 2.5, and the cutoff is exponential. The radius of gyration, R_g, is predicted to increase with the molar mass of the branched macromolecules following a power law

$$R_g \propto M^{1/d_f} \tag{2}$$

where d_f is the so-called fractal dimension. Mean field theory predicts $d_f = 4$, which implies that the density of the branched PU macromolecules increases linearly with the size. This result is, of course, unphysical when the density approaches unity. Clearly, for large macromolecules, one cannot neglect the effects of cyclization and excluded volume interactions. Many refinements of the theory[6] have been developed which include for instance small cycles,[7] but all lead to unphysical results close to the gel point.

A very different approach for the description of the system close to gel point is the percolation model.[8,9] Computer simulations of this model also show a power law dependence of $N(M)$ and R_g but with different values of the exponents: $\tau = 2.2$ and $d_f = 2.5$. Unfortunately, these scaling predictions are useful only very close to the gel point and for $M \gg M_0$. The critical values of r and p and the molar mass distribution at small M depend on the details of the simulation procedure. To obtain realistic computer simulations, one needs to consider reactivity, mobility, flexibility, and interactions. At the moment, such simulations are not feasible. Therefore, mean field theory continues to play a role in the description of gelling systems not too close to the gel point.

Molar mass distributions of a number of gelling systems have been investigated using size exclusion chromatography (SEC). In early investigations, attention was focused on the fraction of the first few oligomers, and the results were found to be in good agreement with mean field theory.[10−12] More recently, the results for high M were found to be close to the scaling prediction of the percolation model.[13−16] The aim of the present paper is to investigate for one system the full molar mass distribution during the whole gelation process and to study the range of M over which either mean field theory or the percolation model can be applied. We also investigate the linear system for which mean field theory is expected to give a good description over the whole range of r.

10.1021/ma9901543 CCC: $19.00
Published on Web 02/02/2000

Theory

A detailed discussion of mean field theory can found in refs 5 and 17. In this paper we investigate the polycondensation of n_B moles of a polyol (B) with functionality φ_B and molar mass M_B and n_A moles of a diisocyanate (A) ($\varphi_A = 2$) and molar mass M_A. The number and weight-averaged molar masses of the starting material are M_{no} and M_{wo} respectively:

$$M_{n0} = \frac{r\varphi_B M_A + 2M_B}{2 + r\varphi_B} \quad M_{w0} = \frac{r\varphi_B M_A^2 + 2M_B^2}{r\varphi_B M_A + 2M_B} \tag{3}$$

The composition of the macromolecules formed by the reaction can be characterized by the number of monomers A (m_A) and B (m_B). As we vary the stoichiometric ratio $r = \varphi_A n_A/\varphi_B n_B$, keeping $r < 1$ and allowing the reaction to go to completion, it follows that $m_B = m_A + 1 = m$ and the reaction extent measured in alcohol groups is r. In this particular case the molar fraction of macromolecules with a particular composition m is given by

$$N(m) = \frac{2r\varphi_B[m(\varphi_B - 1)]!}{(2 - r\varphi_B)m!(m\varphi_B - 2m + 2)!} r^{m-1}(1 - r)^{m\varphi_B - 2m + 2} \tag{4}$$

For large m, $N(m)$ decreases with increasing m following a power law dependence:

$$N(m) \propto m^{-2.5}\exp(-m/m^*) \quad m \gg 1 \tag{5}$$

The distribution has an exponential cutoff at a characteristic size m^* which is proportional to the z-average degree of polymerization (m_z). m^* diverges at the critical value of r: $r_c = (\varphi_B - 1)^{-1}$.

The weight fraction is

$$W(m) = N(m)\frac{(2 - r\varphi_B)[mM_B + (m - 1)M_A]}{(2 + r\varphi_B)M_{n0}} \tag{6}$$

The number and weight-averaged molar masses are given by

$$M_n = M_{n0}\frac{2 + r\varphi_B}{2 - r\varphi_B}$$

$$M_{w0} = M_{w0}\frac{2r\varphi_B[r(\varphi_B - 1)M_A^2 + M_B^2 + 2M_A M_B]}{(2 + r\varphi_B)[(1 - r(\varphi_B - 1)]M_{n0}} \tag{7}$$

Properties of percolation are discussed in ref 8. The number distribution of macromolecules with m monomers close to, but before, the gel point has been obtained using 3-d Monte Carlo simulations:[18]

$$n(m) \propto m^{-2.19}\exp\left[-\left(\frac{(m/m_z)^{0.45} - 0.521}{0.763}\right)^2\right] \quad m \gg 1 \tag{8}$$

The cutoff function is close to an exponential for $m \gg m_z$ but peaks at $m \approx m_z$. The number distribution at large m is independent of the small-scale structure and thus is not influenced by the details of the simulation method. However, the properties of $n(m)$ at small m and the critical connectivity extent depend strongly on these details.

Experimental Section

Sample Preparation. Polyurethanes were formed by condensation of poly(oxypropylene) with hexamethylene diisocyanate (HMDI). Branched PU was obtained using a three-armed POP triol while linear PU was obtained using POP diol. The polyols used in this study are propylene oxide adducts of trimethylolpropane kindly provided by Arco. We used POP triol with three different number-averaged molar masses—T260, M_n = 260 g/mol, M_w/M_n = 1.1; T720 g/mol, M_n = 721, M_w/M_n = 1.08; and T2500, M_n = 2590 g/mol, M_w/M_n = 1.1—and one POP diol—D425, M_n = 426 g/mol, M_w/M_n = 1.06. The samples have been characterized in detail by a number of techniques.[19] In general, the amount of material with functionality less than 3 for POP triols and less than 2 for POP diols increases with increasing molar mass. It is negligible for T260, T720, and D425 (<1%), but the sample T2500 contains a few percent (<5%) material with functionality 1. POP was carefully dried under vacuum, and 2×10^{-3} g dibutyl tin dilaurate catalyst was added for every gram of HMDI. After mixing and complete homogenization of the reaction components, the samples were cured at 40 °C until complete consumption of the isocyanate groups. Samples at different connectivity extents were prepared by varying the ratio of isocyanate groups to hydroxyl groups. The samples were analyzed after dilution in THF. Samples that contained a gel fraction were filtered through 0.45 μm pore size Millipore filters.

Light Scattering. Light-scattering measurements were made using an ALV-5000 multibit multi-τ correlator in combination with a Malvern goniometer and a Spectra Physics argon ion laser operating with vertically polarized light with wavelength $\lambda = 532$ nm. The range of scattering wave vectors covered was $3.0 \times 10^{-3} < q < 3.5 \times 10^{-2}$ nm^{-1} with $q = (4\pi n_s/\lambda)\sin(\theta/2)$, θ being the angle of observation. The temperature was controlled by a thermostat bath within ±0.1 °C.

Size Exclusion Chromatography. We used a classical analytical SEC apparatus with eluent THF. For linear PU a single PL-Gel column was used (Polymer Laboratories MIX-C 5 μm, 600 × 7.5 mm) while for branched PU two PL-Gel columns (Polymer Laboratories E-lin 10 μm and MIX-B 10 μm, each 600 × 7.5 mm) were used in series. The distribution of branched PU extends to very high molar masses ($M > 10^7$ g/mol). Although branched, these large macromolecules are sensitive to shear-induced degradation. Therefore, we removed the filter and the precolumn that usually protect the columns against pollution. The influence of the concentration and the flow rate was checked. The chromatograms shown below were obtained using concentrations of a few milligrams per milliliter and a flow rate of 0.5 mL/min for branched PU and 1 mL/min for linear PU. Choosing a flow rate larger than 0.5 mL/min leads to distortion of the high molar mass tail of branched PU. Even at 0.5 mL/min, some degradation still occurs, but only for very large macromolecules beyond the resolution of the columns.

The concentration was monitored by a differential refractometer (R410 from Millipore—Waters). To obtain the correct value of the concentration we need to know the refractive index increment (dn/dC) as a function of the retention volume (V_R). dn/dC varies both with the molar mass of the precursor POP and with the connectivity extent due to the influence of end groups and urethane links. The variation of dn/dC with the molar mass of the precursors is weak and becomes negligible for $M > 2000$ g/mol. The variation of dn/dC with the connectivity extent becomes negligible for larger oligomers because the number urethane links per POP segment becomes constant.

We can calculate the dependence of dn/dc on the connectivity extent, if we assume that, starting from the tetramers, branched POP has a constant dn/dc independent of the molar mass. The value of dn/dC of the first three oligomers was deduced from the experimental chromatographs in the following way. Let the values of dn/dC of the monomer, dimer, trimer

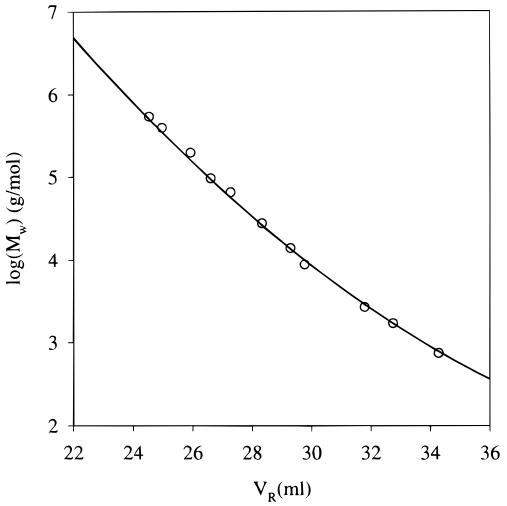

Figure 1. Calibration curve of branched PU based on T720. The solid line represents the result of a least-squares fit: $\log(M_w) = 19.74 - 0.776V_R + 7.97 \times 10^{-3}V_R^2$.

and *n*-mer with $n > 3$ be x1, x2, x3 and x*n*. The relative area on the chromatographs corresponding to the first three oligomers (A1, A2, A3) was obtained by fitting to a sum of exponentially modified Gaussian functions. The relative area of the larger polymers (A*n*) is simply A$n = 1 - A1 - A2 - A3$. The average value of d*n*/d*C* ($\langle x \rangle$) is obtained from the integrated refractive index signal and the total mass of the material injected in the columns and is equal to $\langle x \rangle = A1(x1) + A2(x2) + A3(x3) + An(xn)$. The value of x1 is determined by measuring the starting product. The value of x*n* is determined from measurements of samples that contain only a small fraction of the first three oligomers. The two remaining unknowns can be obtained from measurements at small values of *r*. In principle two measurements are enough, but we have used four measurements which gave consistent results. In this way we obtained for T720, x1 = 0.053, x2 = 0.060, x3 = 0.063, and x*n* = 0.065; for T260, x1 = 0.053, x2 = 0.070, x3 = 0.076, and x*n* = 0.084; and for D425: x1 = 0.043, x2 = 0.060, x3 = 0.063 and x*n* = 0.069. A posteriori, we note that the neglect of the variation of d*n*/d*c* of the larger oligomers leads to an error of at most a few percent. For T2500 the effect of connectivity on d*n*/d*c* is negligible.

Molar mass distributions were determined by transforming V_R into the corresponding molar mass using calibration curves. The calibration curve of branched PU based on T720 was obtained by collecting fractions at different values of V_R The fractions had a polydispersity index $M_w/M_n \approx 1.2$. The mass averaged molar mass of the fractions was determined from the *q*-dependent scattering intensity using the Zimm approximation;[20] see Figure 1. The concentration of the samples was sufficiently low so that interaction could be neglected. The molar mass of linear PU was found to be proportional to that of polystyrene at the same V_R: $M_{PU} = 0.7M_{PS}$. The refractive index values were transformed into concentrations using the molar mass dependence of the refractive index. The latter was obtained by a smooth interpolation between the discrete values obtained for the first three oligomers and assuming a constant value at low and high molar masses given by x1 and x*n*, respectively. The concentration as a function of *M*, or log(*M*) was calculated from the concentration as a function of V_R as follows:

$$C(M) = \frac{C(V_R)\,dV_R}{dM} \quad \text{or} \quad C(\log(M)) = \frac{C(V_R)\,dV_R}{M\,d\log M} \qquad (9)$$

Results

Figure 2 shows chromatograms of branched PU based on POP triol T720 at different values of *r*. $r_c = 0.569$ was determined using mechanical measurements.[21]

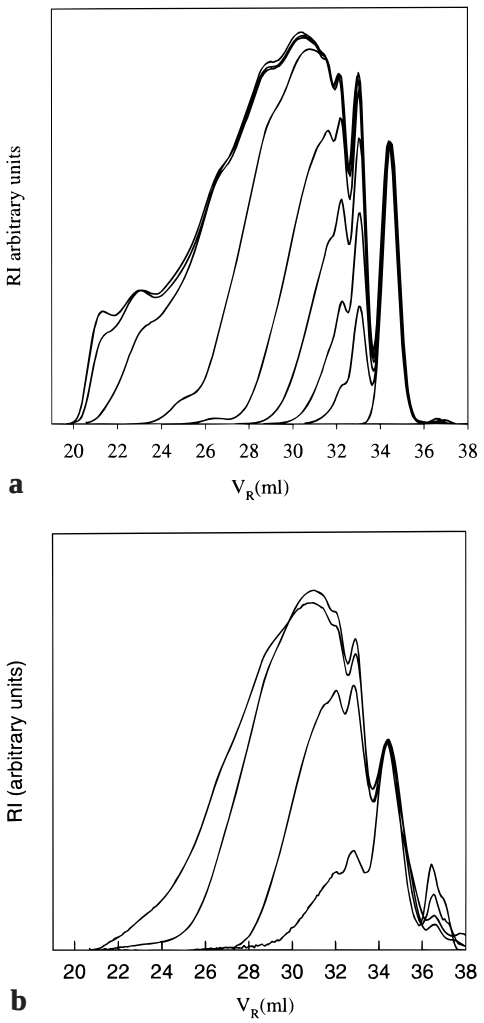

Figure 2. Chromatographs of branched PU based on T720 at various values of *r* below (a) and above (b) the gel point. For clarity the data were normalized so that the peaks of the monomer coincide. Below the gel point (a) the distribution becomes larger with increasing *r*: 0, 0.1, 0.2, 0.3, 0.4, 0.5, 0.55, 0.56, and 565. Above the gel point (b) the distribution becomes narrower with increasing *r*: 0.57, 0.6, 0.7, and 0.8.

With increasing *r*, the molar mass distribution broadens, and very close to r_c, the largest macromolecules are no longer separated but all exit the columns at the volume of total exclusion. We can distinguish the monomer, dimer, and trimer, but at higher *M* the distribution becomes continuous. The shape and position of the peaks corresponding to the first three oligomers do not vary significantly with *r*. Weight fractions of the first three oligomers were deduced from the area of the peaks corresponding to each oligomer; see Experimental Section.

The results are shown in Figure 3 together with the prediction from mean field theory. The mean field calculation describes the experimental data well at small *r*, but systematically underestimates the data at larger *r* especially for the trimer. However, the determination of the peak area of the trimer is uncertain due to the overlap with larger oligomers.

Figure 4 shows chromatograms of linear PU based on POP diol D425 at different values of *r* up to $r = 1$. In contrast to PU based on POP triol, the distribution does not become very broad, but the maximum moves to lower retention volume with increasing *r*. The fraction of the first three oligomers is compared with mean field

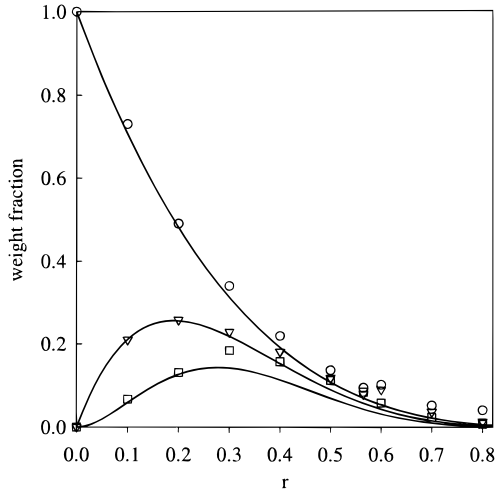

Figure 3. Weight fractions of the monomer (circles), dimer (triangles), and trimer (squares) of branched PU based on T720 as a function of *r*. The solid lines represent predictions of mean field theory.

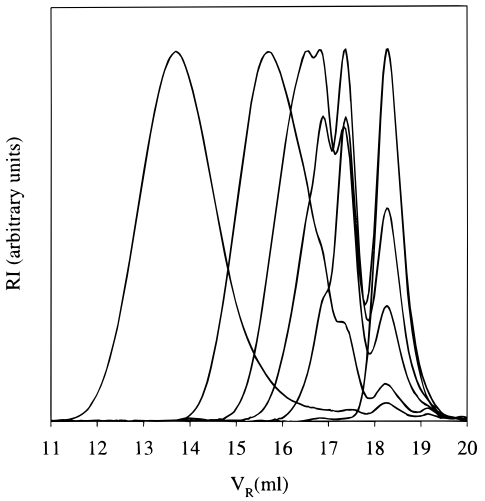

Figure 4. Chromatograms of linear PU based on D425 at various values of *r*. For clarity the data are normalized by the maximum signal. The distribution shifts to smaller values of V_R with increasing *r*: 0, 0.2, 0.4, 0.6, 0.8, and 1.0.

calculation in Figure 5. The mean field prediction is consistent with the experimental data.

To show the generality of these results we have done experiments up to the gel point with T260 and T2500 using the same method; see Figure 6. Again agreement with mean field calculations is obtained at small *r* with a systematic deviation at larger *r*. Of course, the higher the molar mass of the precursors, the more difficult it is to distinguish the oligomers, which might explain the somewhat stronger deviation of the data with the theory for T2500.

It appears that mean field theory predicts the evolution of the weight fractions of at least the first three oligomers reasonably well considering the experimental error, but does it do equally well for the higher molar masses? For linear PU mean field theory predicts that the molar mass diverges as $r \rightarrow 1$. In fact we observe a finite molar mass for the sample that was prepared to give $r = 1$. However, small deviations of *r* from unity or a small fraction of material with functionality less than 2 can easily lead to the value found in the experiment, see below. Similar arguments can be raised to explain why the critical reaction extent for gelation is larger

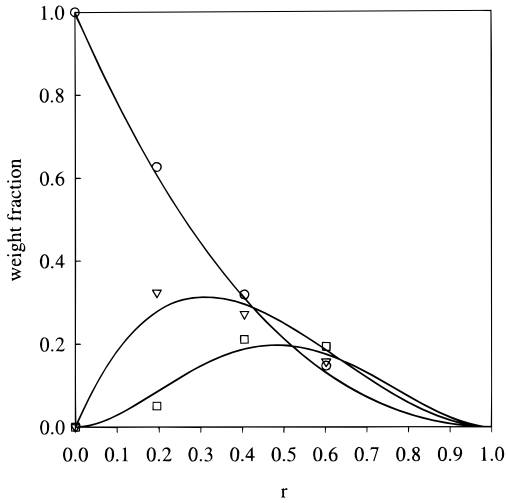

Figure 5. Weight fractions of the monomer (circles), dimer (triangles), and trimer (squares) of linear PU based on D425 as a function of *r*. The solid lines represent predictions of mean field theory.

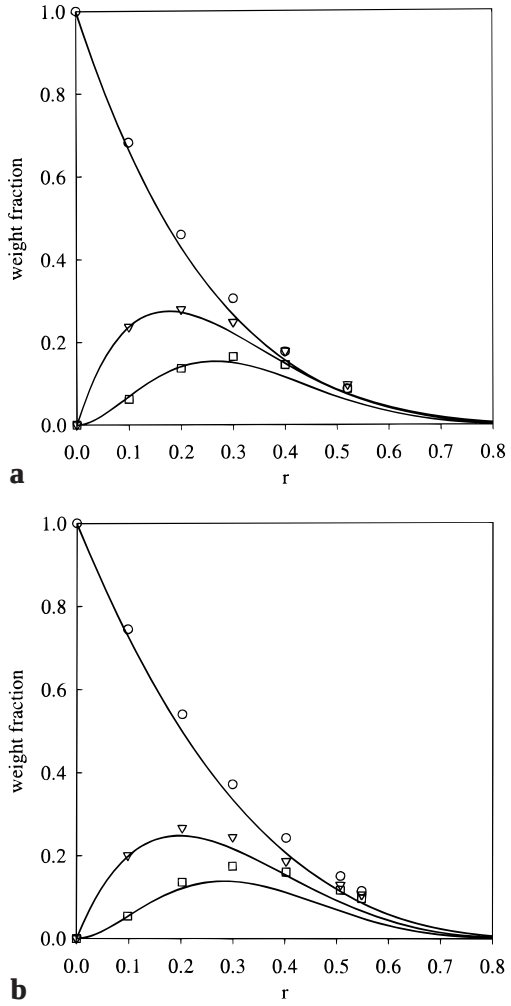

Figure 6. (a) Weight fractions of the monomer (circles), dimer (triangles), and trimer (squares) of branched PU based on T260 as a function of *r*. The solid lines represent predictions of mean field theory. (b) Weight fractions of the monomer (circles), dimer (triangles) and trimer (squares) of branched PU based on T2500 as a function of *r*. The solid lines represent predictions of mean field theory.

than the value predicted by mean field theory: $r_c = 0.5$. For PU based on T260, T720, and T2500 we find $r_c =$

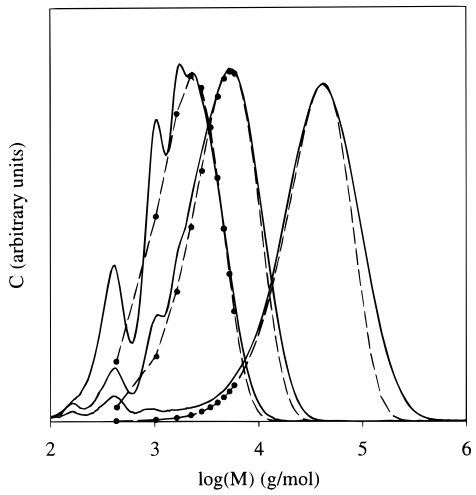

Figure 7. Molar mass distributions of linear PU based on D425 at $r = 1$, 0.8, and 0.6. For clarity the data are normalized by the maximum signal. The dashed lines represent predictions of mean field theory. Values predicted for the first 10 oligomers are indicated by dots.

0.52, 0.569, and 0.58, respectively. An additional cause of retardation of the gel point is cyclization, which is much more likely for branched than for linear PU.

We have done a detailed study of the molar mass distribution at different values of r for linear PU based on D425 and branched PU based on T720. Figure 7 shows the molar mass distributions of linear PU based on D425 for three values of r: 0.6, 0.8, and 1. The experimental results are compared with mean field calculations. For the case where we aimed for $r = 1$, we found the best agreement with mean field calculations using $r = 0.972$. A very similar calculated result is obtained if we assume a small fraction of mono functional POP,[5,17] although for the samples used here this fraction is negligible. There is good general agreement, but small systematic deviations can be observed. The calculations for the samples at $r = 0.8$ and $r = 0.972$ underestimate the high molar mass fraction. In addition, the relative amount of small oligomers is larger than predicted. This is especially evident for $r = 0.972$ for which the fraction of the first few oligomers is clearly not negligible as predicted by mean field theory. The two effects could be correlated because a lower reactivity of small polymers leads to a relatively larger fraction of large polymers. Note the presence of a very small fraction with molar mass about halve that of the precursor. This material is probably a contaminant of the precursor and is inert, as the amount stays constant throughout the reaction.

Figure 8 shows the molar mass distributions of branched PU based on T720 for three values of r close to r_c: 0.55, 0.56, and 0.565. The molar mass distribution of the three samples is the same for small M as expected from the small change in r. The difference at high M is due to the divergence of M_w at r_c. In Figure 8, the experimental results are compared with the predictions of mean field theory and the percolation model at the gel point. Mean field theory gives a good description of the distribution at low molar mass for $M < 1.3 \times 10^4$ g/mol (degree of polymerization DP < 15). The percolation model gives a good description for $M > 3 \times 10^5$g/mol (DP > 320). However, the experimental distribution is not smooth as predicted. We do not know whether the undulations are an artifact of the column separation

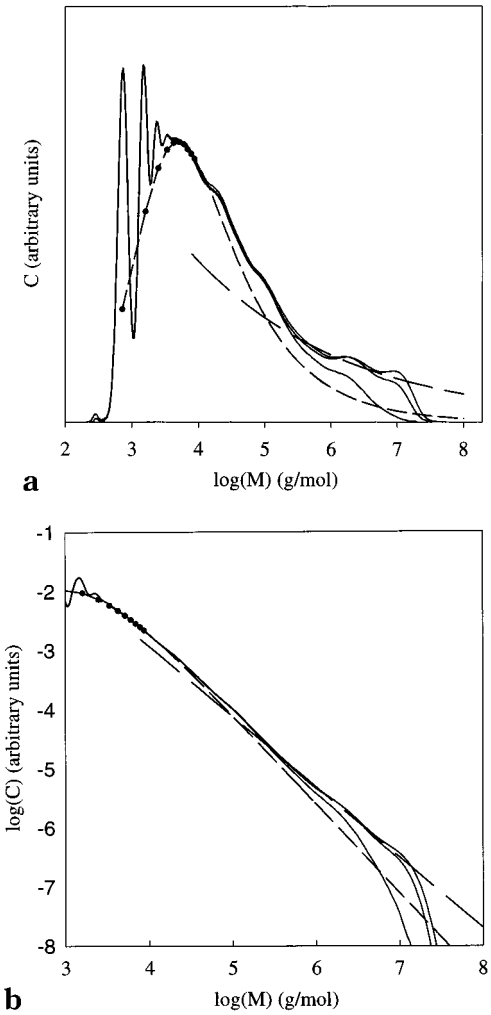

Figure 8. (a) Molar mass distributions of branched PU based on T720 at $r = 0.565$, 0.56, and 0.55. For clarity the data were normalized so that the peaks of the monomer coincide. The short dashed line represents the prediction of mean field theory at the gel point. Values predicted for the first 10 oligomers are indicated by dots. The long dashed line represents the scaling behavior at high M of the percolation model. (b) Double logarithmic representation of the same data as in Figure 8a.

or characteristic of the distribution. Similar effects were observed for other gelling systems.[13,14,16] If the undulations are due to an artifact, it must be related to the branched structure of the macromolecules as the distributions of large linear PU are perfectly smooth.

The SEC columns used in the experiment do not correctly separate macromolecules with $M > 3 \times 10^6$ g/mol. This means that the molar mass distribution for the samples with $r = 0.56$ and 0.565 is artificially cut off. The true cutoff function of the molar mass distribution can be observed for the sample at $r = 0.55$ for which a simple exponential cutoff describes the data best. Unfortunately, M^* for this sample is not large enough to be in the regime described by the percolation model. With the SEC columns available today, we cannot check whether the cutoff function of the molar mass distribution very close to the gel point agrees with that of the percolation model given in eq 6.

Figure 9 shows the weight and number-averaged molar masses as a function of r for linear and branched PU. The data are compared with predictions from mean field theory. For linear PU the agreement is good except for the sample at $r = 1$ where M_w is expected to diverge.

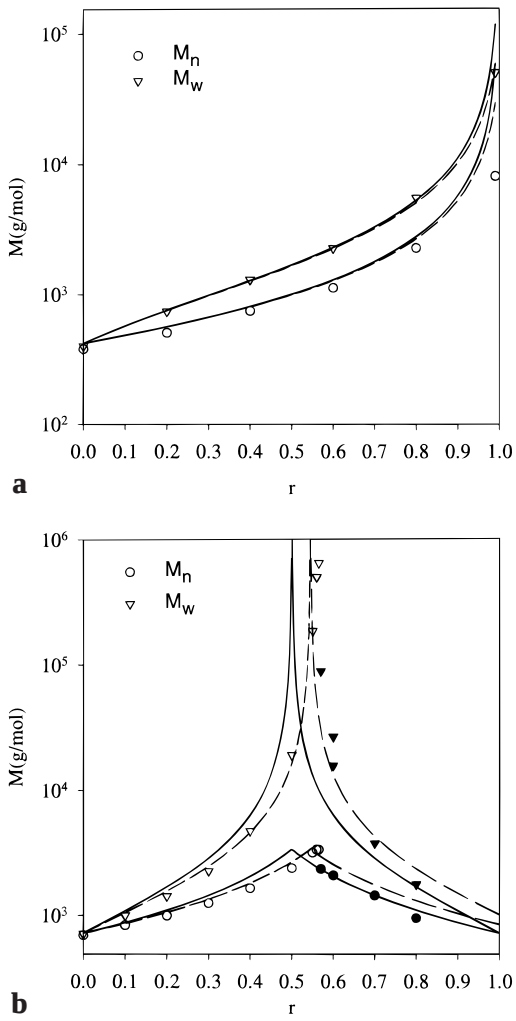

Figure 9. (a) Weight and number-average molar mass of linear PU based on D425 as a function of r. The solid and dashed lines represent predictions of mean field theory assuming that the true value of r is the measured value or is smaller by 3%, respectively. (b) Weight and number-average molar mass of branched PU based on T720 as a function of r. Filled symbols are used for samples that contained a gel fraction. The solid and dashed lines represent predictions of mean field theory assuming that the true value of r is the measured value or is smaller by 9%, respectively.

A good agreement with the experimental value of M_w is obtained if we assume that the real value of r is slightly less than 1. The value of M_n for the largest sample is much less than predicted from mean field theory. This is due to the presence of a small amount of oligomers even at r close to 1, see Figure 7, that weigh heavily in the calculation of M_n.

M_w of branched PU diverges at $r = 0.57$ and not at $r = 0.5$ as predicted by mean field theory. Note that the values of M_w at $r = 0.56$ and especially at $r = 0.565$ are underestimated due to the limited resolution of the SEC columns. We can improve the comparison by assuming that the real value of r is smaller by 9%, but we cannot obtain a correct description of M_w over the whole range of r in this way. However, mean field theory can describe the dependence of M_n correctly. This is expected because M_n is sensitive to the distribution at small M for which mean field theory gives a good approximation while M_w is sensitive to the distribution at high M where mean field theory fails. At large r, the total amount of soluble material becomes small, and the results are sensitive to traces of material that are nonfunctional, which leads to lower averaged molar masses.

Discussion

It appears that mean field theory gives a good description of the molar mass distributions of linear and branched PU as long as the degree of polymerization is less than approximately 15. This means that mean field theory can be used to describe the properties of gelling systems for $r < 0.8r_c$ and $r > 1.2r_c$. For DP larger than about 300, the molar mass distribution is compatible with the scaling behavior of the percolation model. In 3d Monte Carlo simulations of site percolation we found that the scaling behavior is reached at about the same degree of aggregation.[18] The percolation model is therefore useful only in a very small range: $0.95r_c < r < 1.05r_c$. This observation is in agreement with mechanical shear measurements on the same system.[21] The percolation model in conjunction with the assumption of Rouse dynamics predicts a power law frequency dependence of the shear modulus. The predicted power law dependence was indeed observed, but only very close to r_c and only at frequencies much lower than those at which the precursors relax.

In earlier SEC studies of gelling systems, it was assumed that the limiting power law dependence of the molar mass distribution is reached already for relatively low degrees of polymerization. Such an analysis gives a good description of the data at least in a log−log representation as shown in Figure 8b. For the present system such an analysis gives $\tau = 2.3$. This value and those found for other systems[13−16] are only slightly larger than the value found in computer simulations of percolation and give the wrong impression that the percolation model is correct already for small degrees of polymerization. In fact, most of the molar mass range observable by SEC is situated in the crossover regime. A similar conclusion was reached by Colby et al. for branched polyesters.[22]

In principle, it is possible to determine the fractal dimension of the branched polymers from the scattering wave vector (**q**) dependence of the scattered light or from the molar mass dependence of the radius of gyration. If we want to measure d_f of percolating clusters these measurements need to be done on large clusters, i.e., percolating clusters, and on large length scales, i.e., at q^{-1} larger than the size of the smallest percolating clusters. Such large values of q^{-1} can be reached with light scattering, but light-scattering measurements need to be done on highly diluted systems. Unfortunately, the fractal dimension of clusters swollen in a good solvent is not directly related to d_f in the original system.[23] In addition, polydispersity influences the measured value: $d_f(\text{mono}) = (3 - \tau)d_f(\text{poly})$ if $\tau > 2$. A comparison between the results on polydisperse systems and monodisperse fractions could therefore yield a value for τ. Such measurements have been attempted using SEC to prepare monodisperse fractions.[24,25] However, only an apparent value of τ was obtained as the molar mass range of the monodisperse fractions is clearly in the transition regime.

The conclusion from this work is that it is difficult to reach the regime where the percolation model is valid. This conclusion is even more pertinent for most other systems studied in the literature for which the elementary unit is larger than that of the branched PU studied here. A look at the literature shows that almost all

investigations of gelling systems were done in the crossover regime. Often scaling relations were obtained with data that included results on oligomers. The situation is similar to early investigations of critical exponents governing phase transitions.[26] More attention should be given to describe the important transition regime where both mean field theory and the percolation model fail.

Acknowledgment. We thank Frederic Foucault and Jean Pierre Busnel for their help with the SEC experiments.

References and Notes

(1) Flory, P. J. In *Principles of Polymer Chemistry*; Cornell University Press: Ithaca, NY, 1953.
(2) Stockmayer, W. H. *J. Chem. Phys.* **1943**, *11*, 45; *J. Chem. Phys.* **1944**, *12*, 125.
(3) Gordon, M. *Proc. R. Soc. London* **1962**, *A268*, 240.
(4) Macosko, C. W.; Miller, D. R. *Macromolecules* **1976**, *9*, 199.
(5) Durand, D.; Bruneau, C. M. *Macromolecules* **1979**, *12*, 1216; *Makromol. Chem.* **1982**, *183*, 1021.
(6) Durand, D. In *Polymer Yearbook*, 3rd ed.; Pethrick, R. A., Ed.; Harwood Acad. Publ.: Langhorne, PA, 1986; p 229.
(7) Kilb, R. W. *J. Chem. Phys.* **1958**, *62*, 969. Dusek, K.; Ilavsky, M. *J. Polym. Sci. C* **1975**, *53*, 74. Stepto, R. F. T. In *Developments in polymerization 3*; Haward, R. N., Ed., Applied Science Publishers Ltd.: London, 1982; p 81.
(8) Stauffer, D.; Aharony, A. *Percolation theory*, 2nd ed.; Taylor & Francis: London, 1992.
(9) de Gennes, P. G. *Scaling concepts in polymer physics*; Cornell University Press: Ithaca, NY, 1979.
(10) Argyropoulos, D. S.; Berry, R. M.; Bolker, H. I. *Macromolecules* **1987**, *20*, 357.
(11) Hélias, P.; Durand, D.; Busnel, J. P.; Bruneau, C. M. *Eur. Polym. J.* **1982**, *18*, 647.
(12) Clarke, N. S.; Devoy, C. J.; Gordon, M. *Br. Polym. J.* **1971**, *3*, 194.
(13) Schosseler, F.; Benoit, H.; Gubisic-Gallot, Z.; Strazielle, Cl.; Leibler, L. *Macromolecules* **1989**, *22*, 400.
(14) Patton, E. V.; Wesson, J. A.; Rubinstein, M.; Wilson, J. C.; Oppenheimer, L. E. *Macromolecules* **1989**, *22*, 1946.
(15) Bauer, J.; Burchard, W. *Macromolecules* **1993**, *26*, 3103.
(16) Degoulet, C.; Nicolai, T.; Durand, D.; Busnel J. P. *Macromolecules* **1995**, *28*, 6819.
(17) Durand, D.; Bruneau, C. M. *Br. Polym. J.* **1979**, *11*, 194; *Br. Polym. J.* **1981**, *13*, 33.
(18) Gimel, J. C.; Nicolai, T.; Durand, D.; Teuler, J. M. *Eur. Phys. J. B* **1999**, *12*, 91.
(19) Foucault, F. Ph.D. Thesis, Le Mans, 1998.
(20) See e.g.: Huglin M. B., Ed. *Light Scattering from Polymer Solutions*; Academic Press: London and New York, 1972.
(21) Nicolai, T.; Randriantoandro, H.; Prochazka, F.; Durand, D. *Macromolecules* **1997**, *30*, 2460.
(22) Colby, R. H.; Rubinstein, M.; Gillmor, J. R.; Mourey, T. H. *Macromolecules* **1992**, *25*, 7180.
(23) Cates, M. E. *J. Phys. Lett. Fr.* **1985**, *46*, 757.
(24) Bouchaud, E.; Delsanti, M.; Adam, M.; Daoud, M.; Durand, D. *J. Phys.* **1986**, *47*, 1273.
(25) Schosseler, F.; Daoud, M.; Leibler, L. *J. Phys. France SI* **1990**, 2373.
(26) See, e.g.: Chu, B. *Dynamic Light Scattering: Applications of Photon Correlation Spectroscopy*; Pecora, R., Ed.; Plenum Press: New York, 1985; Chapter 7.

MA9901543